Translational Oncology 21 (2022) 101429

Contents lists available at ScienceDirect

Translational Oncology

journal homepage: www.elsevier.com/locate/tranon

Original Research

The CtIP-CtBP1/2-HDAC1-AP1 transcriptional complex is required for the transrepression of DNA damage modulators in the pathogenesis of osteosarcoma

Xun Chen [a,c], Qian Zhang [b], Xiaoqian Dang [c], Jinzhu Fan [a], Tao Song [a], Zhong Li [a], Ning Duan [a,*], Wentao Zhang [a,*]

[a] Department of Orthopaedics, Honghui Hospital, Xi'an Jiaotong University, 76 Nanguo Rd, Beilin District, Xi'an, Shaanxi 710054, China
[b] The Department of Surgery Room, Xi'an Daxing Hospital, Xi'an, Shaanxi 710016, China
[c] Department of Orthopaedics, The Second Affiliated Hospital of Xi'an Jiaotong University, Xi'an, Shaanxi 710005, China

ARTICLE INFO

Keywords:
CtIP
CtBP1
CtBP2
AP1, DNA damage
Osteosarcoma

ABSTRACT

Most tumors, including osteosarcomas, have deficiencies in DNA damage repair. However, the regulatory mechanisms underlying dysregulation of DNA damage repair genes are still being investigated. In this study, we reveal that C-terminal binding protein (CtBP) interacting protein (CtIP) couples with three transcriptional regulators, CtBP1/2 heterodimer, histone deacetylase 1 (HDAC1), and two subunits of the activating protein 1 (AP1) transcription factor to assemble a transcriptional complex. This complex specifically controls the expression of four genes involved in DNA damage and repair processes: MutL homolog 1 (*MLH1*), MutS Homolog 3 (*MSH3*), breast cancer type 1 (*BRCA1*), and cyclin dependent kinase inhibitor 1A (*CDKN1A*). Chromatin immunoprecipitation (ChIP) assay results revealed that the CtIP-CtBP1/2-HDAC1-AP1 complex regulated these four genes by binding to their promoters through the TGAT/CTCA consensus sequence. The depletion of CtIP, CtBP1/2, and HDAC1 increased the expression levels of *MLH1, MSH3, BRCA1*, and *CDKN1A* and inhibited *in vitro* and *in vivo* osteosarcoma cell growth. Overexpression of *MLH1, MSH3, BRCA1*, or *CDKN1A* in osteosarcoma cells can reduce cell viability, colony formation, cell migration, and tumor growth. Our findings suggest that the CtIP-CtBP1/2-HDAC1-AP1 complex is required for mediation of DNA damage processes for the pathogenesis of osteosarcoma.

Introduction

Osteosarcoma, a malignant bone tumor, tends to occur in young children, teenagers, and young adults [1,2]. The epidemiology of osteosarcoma is very low worldwide, with an annual global incidence rate of only approximately 5 persons per million [1,2]. The underlying mechanisms that determine the pathogenesis of osteosarcoma are complicated, and osteosarcoma can arise due to many factors, such as dysregulation of oncogenes and tumor suppressor genes, deficiencies in the DNA damage and repair system, activation and impairment of signaling pathways, and microenvironmental effects [3,4]. This wide range of potential triggers suggests that transcriptional regulation is an important process driving osteosarcoma pathogenesis.

One group of transcriptional regulators, the C-terminal binding proteins (CtBPs), coordinate with histone modifying enzymes (e.g., histone deacetylases [HDACs] and histone acetyltransferases [HATs]) and transcription factors [5,6]. CtBP1 and CtBP2 can serve as both corepressors and coactivators, and both are dysregulated in multiple biological processes, such as tumorigenesis, inflammation, and apoptosis [5–7]. CtBPs are involved in the regulation of numerous genes, including breast cancer 1 (*BRCA1*) and *BRCA2*, cyclin dependent kinase inhibitor 1A (*CDKN1A*, also known as *p21*), B-cell lymphoma 2 (BCL2) associated X (*BAX*), BCL2-interacting killer (*BIK*), BCL2 interacting mediator (*BIM*), BCL2 binding components 3 (*BBC3*, also known as *PUMA*), cadherin 1 (*CDH1*), neuronal differentiation 1 (*NEUROD1*), plakophilin 1 (*PKP1*), distal-less homeobox 5 (*DLX5*), and multidrug resistance protein 1 (*MDR1*) [5–7].

Control of a portion of these target genes occurs by different CtBP-associated transcriptional complexes [5–7]; for example, CtBP1 couples with p300 (a HAT) and forkhead box O3a (FOXO3a) to mediate the expression of *BAX, BIM*, and *BIK* in osteosarcoma cells [8]. CtBP1 also assembles a complex with lysine demethylase 1 (LSD1),

* Corresponding authors.
E-mail addresses: duanning07@stu.xjtu.edu.cn (N. Duan), zhangwentao1975@gmail.com (W. Zhang).

https://doi.org/10.1016/j.tranon.2022.101429
Received 18 January 2022; Received in revised form 7 April 2022; Accepted 11 April 2022

p300/CBP-associated factor (PCAF), and RAS-responsive element binding protein 1 (RREB1) to activate the expression of *NEUROD1* in gastrointestinal endocrine cells [9]. It also forms a complex with zinc finger protein 750 (ZNF750), kruppel like factor 4 (KLF4), and repressor element-1 silencing transcription factor corepressor 1 (RCOR1) to control the expression levels of *PKP1* and *DLX5* in the process of epidermal differentiation [10]. The direct interaction between CtBP1 and forkhead box M1 (FOXM1) can induce chemoresistance by transactivating *MDR1* [11].

Another protein, CtBP interacting protein (CtIP), is overexpressed in multiple cancers and is mainly involved in the regulation of DNA repair and in cell cycle control [12]. CtIP associates with the MRE11-RAD50-NBN (MRN, Meiotic Recombination 11/Radiation Sensitive 50/Nibrin) complex to mediate DNA double-strand break (DSB) repair and homologous recombination (HR) repair [13,14]. CtIP also functions as an adapter that interacts directly with both BRCA1 and CtBP1, and the resulting complex further suppresses the expression of *CDKN1A* [15]. The CtBP1/CtIP complex is also recruited by the RBP-Jk/SHARP (recombination signal binding protein 1 kappa J region/silencing mediator of retinoic acid and thyroid hormone receptor/HDAC1-associated repressor protein) to silence Notch target genes [16].

Although CtIP was originally identified as interacting protein of CtBP1, the CtIP-CtBP associated transcriptional complexes are rarely reported. The aim of the present study was to investigate the role of CtIP in the pathogenesis of osteosarcoma and to identify CtIP-CtBP associated protein complex members and their downstream targets. We used CtIP-CtBP deficient cells for *in vitro* phenotype assays and to construct an *in vivo* tumor xenograft model to investigate whether disruption of the CtIP-associated complex could effectively suppress the expression of the downstream targets.

Materials and methods

Cells and cell culture

One human osteoblast cell line (hFOB1.19) and 6 human osteosarcoma cell lines (MG63, KHOS, 143B, HOS, Saos2, and U2OS) were purchased from the American Type Culture Collection (ATCC) in May 2016 (Manassas, VA, USA). All cell lines were tested and authenticated using the short tandem repeat (STR) method upon receipt. All cell lines were cultured in RPMI1640 medium (Sigma-Aldrich, Shanghai, China; #R6504) containing 10% fetal bovine serum (FBS) (Sigma-Aldrich; #12003C) and were maintained in a humidified 5% CO_2 atmosphere at 37 °C (34 °C for hFOB1.19 cells) with medium changes every two days. All cell lines were routinely tested for mycoplasma contamination using the LookOut Mycoplasma qPCR Detection Kit (Sigma-Aldrich, Shanghai, China; #MP0040A). Cell lines were re-examined to exclude contamination before submission of this manuscript (November 2021).

Construction of vectors

The full-length coding sequences of *CtIP, CtBP1, HDAC1, MLH1* (MutL homolog 1), *MSH3* (MutS Homolog 3), *BRCA1*, and *CDKN1A* were cloned into pCDNA3-Flag empty vector with the BamHI and XhoI sites. The full-length coding sequences of *CtIP, CtBP1*, CtBP2, *HDAC1, JUN* (Jun Proto-Oncogene, AP-1 transcription factor subunit), and *FOS* (Fos Proto-Oncogene, AP-1 Transcription Factor Subunit) were cloned into pCDNA3-Myc empty vectors with the KpnI and XhoI. The primers of all these vectors are listed in Table S1. All vectors were verified by DNA sequencing.

Collection of biopsies

Cancerous biopsies and their adjacent noncancerous tissues were collected from osteosarcoma patients ($n = 20$) who were all diagnosed as stage III. These patients were all diagnosed and underwent surgery in the Department of Orthopedics, Xi'an Honghui Hospital. All participants signed a consent form reviewed and approved by the ethical board of Xi'an Honghui Hospital, Shaanxi, China.

Cell transfection

Gene knockdown and overexpression were performed as described previously [17]. For knockdown gene expression using the short hairpin RNA (shRNA) method, lentiviral pLKO.1 vector containing individual shRNA that specifically targeted *CtIP, CtBP1, CtBP2, JUN*, or *FOS* was transfected into cells. The shRNAs were obtained from Sigma-Aldrich, and the clone IDs are shown in Table S2. A scrambled control that did not target any human genes was used as the control. The transfectants were selected with 2 μg/mL puromycin (Sigma-Aldrich; #P8833) and the individual puromycin-resistant cells were collected and expanded. Small interfering RNAs (siRNAs) that specifically targeted *JUN* and *FOS* (Table S2) and different plasmids were transfected into the cells using Lipofectamine 2000 (Invitrogen, Shanghai, China; #11668019). After incubation in RPMI1640 medium for 24 h, the cells were harvested and gene knockdown and overexpression were validated by examining the mRNA and protein levels.

RNA extraction, microarray analysis, and quantitative real-time PCR (qRT-PCR)

Total RNA was extracted using TRIzol reagent (ThermoFisher Scientific, Shanghai, China; #15596026). The purified RNA (1 μg) was used to generate the first-strand cDNA with the RevertAid First Strand cDNA Synthesis Kit (ThermoFisher Scientific; #K1621), according to the manufacturer's instructions. Microarray analysis was performed using a GeneChip Human Genome U133 Plus 2.0 Array (ThermoFisher Scientific, #900466), following the protocol provided by the manufacturer. Gene expression levels were measured by qRT-PCR analyses using a SYBR Green Kit (Sigma-Aldrich; #QR0100-1KT) and the primers listed in Table S3. The relative expression levels were quantified using the $2^{-\Delta\Delta CT}$ method by normalizing to β-Actin.

Immunohistochemistry (IHC) assay

The CtIP protein level in cancerous biopsies and their adjacent noncancerous tissues were detected by IHC assay following a protocol described previously [17]. Briefly, the paraffin-embedded tissues were cut into 5 μm thick sections, and the sections were mounted onto gelatin-coated histological slides. After rehydration, the sections were probed using anti-CtIP (Santa Cruz Biotechnology; #sc-271339) and then stained with a 3,3′-Diaminobenzidine (DAB) Kit (Abcam; #ab64264). Slides were photographed using an inverted TE 2000 wide-field microscope (Nikon, Tokyo, Japan).

Detection of cell viability

Cell viability was determined using a non-radioactive MTT (3-(4,5-dimethylthiazol-2-yl)-2,5-diphenyltetrazolium bromide) kit (Abcam; #ab211091). In brief, cells were seeded into 96-well plates at a density of approximately 1000 cells/well and incubated for 48 h in a 37 °C incubator. The viable cells were determined by measuring the absorbance at OD 590 nm.

Western blot analysis

Cells and clinical biopsies were lysed in a radioimmunoprecipitation assay (RIPA) buffer supplemented with a protease inhibitor cocktail (Sigma-Aldrich; #11836170001). Protein concentrations in total cell extracts were quantified using the Pierce Coomassie Plus Assay Reagent (ThermoFisher Scientific; #23238). Equal amounts of total protein were

loaded onto 12% SDS-PAGE gels. After transferring to PVDF (polyvinylidene fluoride) membranes (ThermoFisher Scientific; #PB9320) and blocking with 5% (w/v) nonfat milk, the proteins were detected by specific antibodies, including anti-CtIP (Santa Cruz Biotechnology; #sc-271339), anti-CtBP1 (Cell Signaling Technology, Shanghai, China; #8684), anti-CtBP2 (Cell Signaling Technology; #13256), anti-HDAC1 (Cell Signaling Technology; #34589), anti-JUN (Abcam; #ab40766), anti-FOS (Abcam; #ab134122), anti-Myc (Santa Cruz Biotechnology; #sc40), anti-Flag (Sigma-Aldrich; #F3165), anti-Actin (Abcam; #ab179467), anti-LSD1 (Abcam; #aab37165), and anti-GAPDH (glyceraldehyde-3-phosphate dehydrogenase) (Sigma-Aldrich; #G9545).

Immunoprecipitation (IP), mass spectrometry, co-immunoprecipitation (Co-IP)

The methods of IP, mass spectrometry, and Co-IP were the same as described previously [17]. In brief, equal weights (0.1 g) of cancerous biopsies from three osteosarcoma patients, who were all under musculoskeletal tumor society (MSTS) stage III, were mixed and lysed in RIPA buffer containing protease inhibitor cocktail to generate a homogenate. Extracts were centrifuged at 13,000 rpm for 10 min at 4 °C, followed by IP procedures using anti-CtIP- and IgG-associated protein A agarose (Abcam; #ab193255). The immunoprecipitated proteins were resolved by sodium dodecyl-sulfate polyacrylamide gel electrophoresis (SDS-PAGE) and stained using the ProteoSilver Plus Sliver Stain Kit (Sigma-Aldrich; #PROTSIL2). Protein bands were analyzed with a hybrid quadrupole-Orbitrap mass spectrometer (ThermoFisher Scientific). The obtained peptides were blasted in the Mascot server (Matrix Science, Boston, MA, USA).

Cells (1×10^7) expressing different combinations of Myc-tagged and Flag-tagged plasmids were lysed in RIPA buffer containing protease inhibitor cocktail. Extracts were centrifuged at 13,000 rpm for 10 min at 4 °C. The supernatant was subjected to Co-IP assays with both anti-Flag magnetic beads (Sigma-Aldrich; #M8823) and anti-Myc agarose (ThermoFisher Scientific; #20168). After incubation at 4 °C for 2 h, the immunoprecipitated proteins were washed five times with RIPA buffer containing protease inhibitor cocktail. The input and output proteins were subjected to western blot analyses by probing with anti-Flag and anti-Myc, respectively.

Colony formation and cell invasion assays

Cells at the exponential growth phase were seeded into 12-well plates at a density of approximately 1000 cells per well. The cells were placed in a 37 °C incubator and cultured for two weeks, with medium changes every three days. Colonies were stained using 0.3% crystal violet (Sigma-Aldrich; #V5265) and then rinsed 5 times with ddH_2O to remove excess dye. Colony numbers were counted using Image J software.

Cell invasion assays were performed using the Boyden chamber assay. In brief, approximately 100,000 cells were diluted in serum-free RPMI1640 medium and then seeded into the upper chambers (Sigma-Aldrich; #ECM550). The lower chambers were filled with RPMI1640 medium containing 10% FBS. After culture for 24 h, the cells in the lower chambers were fixed with methanol and stained using 0.3% crystal violet. The invaded cells were photographed using an inverted TE 2000 wide-field microscope.

Tumor xenograft model

Osteosarcoma cells (5×10^5) were diluted in 100 μL of PBS containing 50% Matrigel (Sigma-Aldrich; #CLS356255) and injected subcutaneously into 6-week-old C57BL/6 mice ($n = 10$ for each cell line). Tumor volumes were monitored every 5 days. Tumor volumes were calculated using the formula: volume=length × width^2/2. Animal experiments were performed following a protocol (HH201909M) reviewed and approved by our Animal Care and Use Committee.

Chromatin immunoprecipitation (ChIP) assay

Cells (5×10^7) were crosslinked with 1% formaldehyde (Sigma-Aldrich; #252549) to covalently stabilize protein-DNA complexes. The cells were lysed in the lysis buffer provided in the Pierce Magnetic ChIP Kit (ThermoFisher Scientific; #26157), then sonicated to shear the DNA to lengths of approximately 500 bp. The resulting products were immunoprecipitated using anti-CtIP, anti-CtBP1, anti-CtBP2, anti-JUN, anti-FOS, and IgG. The input and output DNA were used for qRT-PCR analyses to measure protein occupancies on the promoters of genes, using the primers listed in Table S4.

Statistical analysis

All experiments in this study were independently performed at least three times. The data were presented using mean ± SD (standard deviation) from at least three independent experiments. For comparisons of mRNA, protein, and ChIP occupancy levels, statistical analyses of data were performed using a two-sided Student's *t* test. For analyses of cell viability and tumor volumes, analysis of variance (ANOVA) was performed, and Duncan's multiple comparison test was used to evaluate differences between different group of cells and mice. Significance was set at $P < 0.05$. All data were generated using GraphPad Prism software (version 8).

Results

CtIP was overexpressed in osteosarcoma cell lines and tumor biopsies

CtIP is overexpressed in several kinds of tumors, such as colorectal and gastric cancers [15,18]. We investigated *CtIP* expression pattern in osteosarcoma by collecting 20 pairs of cancerous biopsies and their adjacent noncancerous tissues from osteosarcoma patients who were all diagnosed as stage III. The *CtIP* mRNA levels were significantly elevated in the cancerous tissues compared to controls (5.74 ± 1.46 vs. 1.87 ± 0.52; tumor tissues vs. controls) (Fig. 1A). We also observed a consistent increase in the CtIP protein levels in three representative cancerous biopsies compared to noncancerous controls (Fig. 1B,C). We also performed IHC assays to determine the CtIP protein levels and again confirmed an elevation in CtIP in tumor biopsies (Fig. 1D).

We used the clinical dataset of osteosarcoma from The Cancer Genome Atlas (TCGA) to evaluate the clinical significance of lower and higher expression levels of CtIP by generating Kaplan-Meier survival curves. The overall survival rate was much worse for patients with high CtIP levels than with low CtIP expression levels (Fig. 1E). We examined the *in vitro* expression levels of CtIP in 6 osteosarcoma cell lines (MG63, KHOS, 143B, HOS, Saos2, and U2OS) and we again consistently found overexpression of CtIP at both the mRNA and protein levels in all 6 cell lines (Figs. 1F,G and S1). Of the 6 cell lines, Saos2 harbored the highest level of CtIP, followed by U2OS, HOS, MG63, KHOS, and 143B (Figs. 1F, G and S1).

Forced expression of CtIP in osteoblast cells could result in tumorigenesis

The observation that overexpression of CtIP is prevalent in different tumor cells [15,18] prompted us to investigate whether forced expression of CtIP in noncancerous osteoblast cells could cause tumorigenesis. We generated two CtIP-overexpression (OE) cell lines (#1 and #2) in the hFOB1.19 background by transfection of pCDNA3-Flag-CtIP. The CtIP mRNA and protein levels in these two OE cell lines both showed a comparable level to that observed in U2OS cells, but they were slightly lower than in Saos2 cells (Fig. 2A–C).

We used the CtIP-OE cell lines, together with hFOB1.19, U2OS, Saos2, and MG63 cells, to perform *in vitro* MTT assays and found that

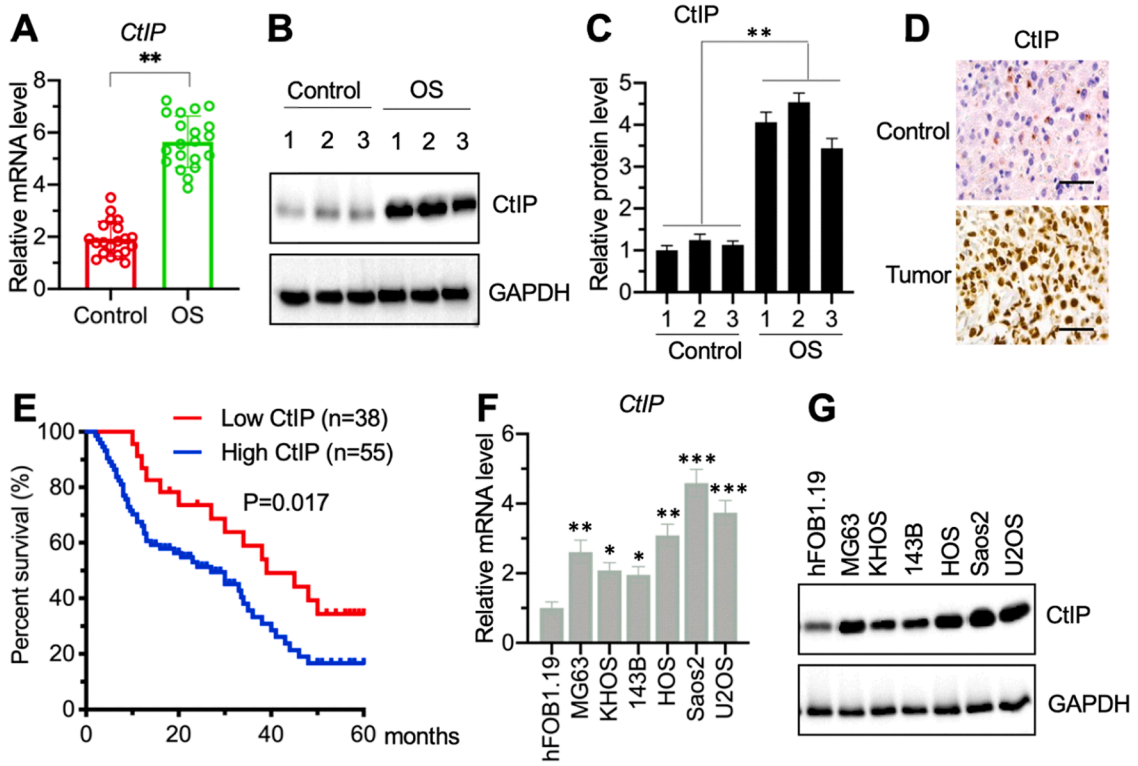

Fig. 1. *CtIP was overexpressed in osteosarcoma tumor biopsies and cells* **(A)** *CtIP* mRNA levels in tumor biopsies (OS) ($n = 20$) and their adjacent noncancerous tissues (Control) ($n = 20$). The data represented the mean values of three independent experiments. $^{**}P < 0.01$. **(B** and **C)** CtIP protein levels in three representative tumor biopsies (OS) and their adjacent noncancerous tissues (Control). **(B)** Western blot results (one representative blot from three independent experiments is shown); **(C)** Quantitative results. $^{**}P < 0.01$. **(D)** IHC results by staining with anti-CtIP in a tumor tissue and its adjacent noncancerous tissue (Control). One representative IHC from three samples is shown. **(E)** Kaplan-Meier survival curves. Osteosarcoma tumor samples harboring high and low levels of CtIP in the TGCA database were analyzed to examine survival rates using Kaplan-Meier plots. **(F** and **G)** *CtIP* mRNA and protein levels in hFOB1.19 cells and 6 osteosarcoma cell lines (MG63, KHOS, 143B, HOS, Saos2, and U2OS). **(F)** qRT-PCR results, $^{*}P < 0.05$, $^{**}P < 0.01$, and $^{***}P < 0.001$; The qRT-PCR data represented the mean values of three independent experiments. **(G)** Western blot results. One representative blot from three independent experiments is shown.

forced expression of CtIP in hFOB1.19 cells significantly increased cell viability compared to the maternal hFOB1.19 cell line (Fig. 2D). The OD_{590} values of two CtIP-OE cell lines were like those in three osteosarcoma cell lines at all examined time points (0, 24, 48, 72, 96, and 120 h) (Fig. 2D).

We also injected the same cell lines into C57BL/6 mice to generate tumors. At 35 days after injection, mice harboring CtIP-OE cells started to form tumors. By contrast, mice injected with hFOB1.19 cells did not produce tumors at any time point (Fig. 2E). The tumor volumes were much smaller in mice injected with CtIP-OE cells than in mice injected with osteosarcoma cells (U2OS, Saos2, and MG63) (Fig. 2E).

CtIP assembled a complex with CtBP1/2, HDAC1, and AP1 transcription factor

We next performed IP assays in the homogenates of three pooled osteosarcoma biopsies (MSTS stage III) using anti-CtIP- or IgG-associated protein A agarose. The purified CtIP-interacting proteins were analyzed by mass spectrometry, and we obtained 67 candidate proteins that might directly or indirectly interact with CtIP (Table S5). Our search for candidate proteins with previously reported involvement in gene transcription regulation identified CtBP1/2, HDAC1, and two subunits (JUN and FOS) of the AP1 transcription factor were highly abundant (Table S5).

Several publications have shown that CtBPs can interact with HDAC1 [19–21]. Moreover, AP1 can also recruit HDAC1 to suppress the expression of matrix metalloproteinase 9 (*MMP9*) [22]. Thus, CtIP quite possibly can form a complex with CtBP1/2, HDAC1, and AP1. We tested this possibility by performing immunoblot assays using the same IP products determined by mass spectrometry analysis, and we confirmed that CtIP could pull down CtBP1/2, HDAC1, JUN, and FOS (Fig. 3A).

We explored how these proteins assembled a complex by constructing pCDNA3-Flag-CtIP, pCDNA3-Myc-CtBP1, pCDNA3-Myc-CtBP2, pCDNA3-Myc-HDAC1, pCDNA3-Myc-JUN, and pCDNA3-Myc-FOS vectors. We co-transfected pCDNA3-Flag-CtIP with individual Myc-tag plasmids, and subsequent Co-IP assays showed that Flag-CtIP could pull down Myc-CtBP1 and Myc-CtBP2, but not the Myc-HDAC1 or Myc-AP1 subunits (Fig. 3B). Co-IP assays after transfection with pCDNA3-Flag-CtBP1 and pCDNA3-Myc (empty vector), pCDNA3-Myc-CtIP, pCDNA3-Myc-CtBP2, pCDNA3-Myc-HDAC1, pCDNA3-Myc-JUN, or pCDNA3-Myc-FOS revealed that Flag-CtBP1 could pull down Myc-CtIP, Myc-CtBP2, and Myc-HDAC1 subunits, but not Myc-AP1 (Fig. 3C). Co-transfection of pCDNA3-Flag-HDAC1 with pCDNA3-Myc, pCDNA3-Myc-CtIP, pCDNA3-Myc-CtBP1, pCDNA3-Myc-CtBP2, pCDNA3-Myc-JUN, or pCDNA3-Myc-FOS verified that Flag-HDAC1 could pull down the Myc-CtBP1/2 and Myc-AP1 subunits, but not Myc-CtIP (Fig. S2A). Thus, we demonstrated that AP1 subunits first recruited HDAC1, which could then interact with the CtBP1/2 heterodimer. CtBP1/2 subsequently bound to CtIP, forming the CtIP-CtBP1/2-HDAC1-AP1 complex (Fig. S2B).

Knockdown of CtIP, CtBP1/2, HDAC1 and AP1 subunits in osteosarcoma cells decreased cell viability, colony formation, cell invasion, and tumor volumes

The deficiency of CtBP1 in osteosarcoma cells significantly decreases cell viability *in vitro* and inhibits tumor growth *in vivo* [11]. We investigated the *in vitro* and *in vivo* effects of CtIP-CtBP1/2-HDAC1-AP1

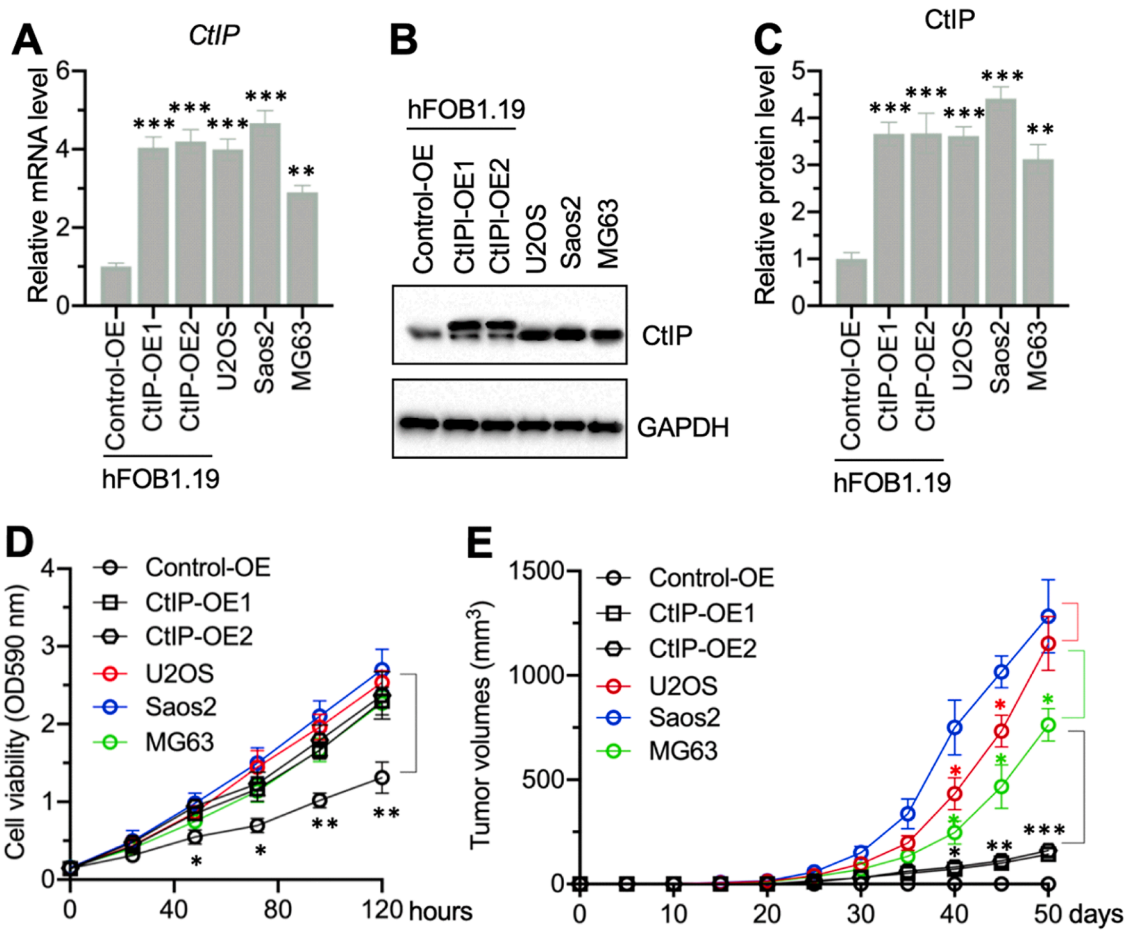

Fig. 2. *Forced expression of CtIP in hFOB1.19 cells increased cell viability in vitro and caused tumorigenesis in vivo* **(A)** *CtIP* mRNA levels in CtIP-OE cells. $^{**}P < 0.01$ and $^{***}P < 0.001$. **(B** and **C)** CtIP protein levels in CtIP-OE cells. **(B)** Western blot results (One representative blot from three independent experiments is shown); **(C)** Quantitative results, $^{**}P < 0.01$ and $^{***}P < 0.001$. **(D)** MTT assay results using CtIP-OE cells and three osteosarcoma cell lines (U2OS, Saos2, and MG63). $^{*}P < 0.05$ and $^{**}P < 0.01$. **(F)** Tumor xenograft results using CtIP-OE cells, U2OS, Saos2, and MG63 cells (for each cell line, 10 mice were injected). Tumor volumes were measured at 5-day intervals. $^{*}P < 0.05$, $^{**}P < 0.01$, and $^{***}P < 0.001$. All data in this figure are presented as the mean ± SD of three independent experiments.

component deficiency by generating Control-KD (knockdown) (transfection of pLKO.1 empty vector without targeting any gene) cell lines and two independent CtIP-KD, CtBP1-KD, CtBP2-KD, HDAC1-KD, JUN-KD, and FOS-KD cell lines in the Saos2 background (Figs. S3 and S4). We then used these cell lines to examine cell viability and verified that the depletion of CtIP, CtBP1, CtBP2, and HDAC1 had similar inhibitory effects on cell viability (Fig. 4A). Depletion of either JUN or FOS also caused a decrease in cell viability, but the OD_{590} values were higher in the AP1-KD cells than in the KD cells of CtIP, CtBP1/2, or HDAC1 at 96 and 120 h (Fig. 4A).

Injection of these cell lines into C57BL/6 mice ($n = 10$ for each cell line) generated tumors that did not differ significantly in size in mice harboring CtIP-KD, CtBP1/2-KD, HDAC1-KD, but the tumors generated by those cells were much smaller than those generated by Control-KD cells (Fig. 4B). The tumor volumes were also smaller in mice injected with AP1-KD cells than in mice harboring Control-KD cells, but they were larger than in mice injected with CtIP-KD, CtBP1/2-KD, or HDAC1-KD cells (Fig. 4B).

Colony formation and cell invasion assays using the same cell lines also revealed that the depletion of CtIP, CtBP1, CtBP2, or HDAC1 also decreased the colony formation numbers and cell invasion capacity; these were much lower than in the Control-KD cells and slightly lower than in the AP1-KD cells (Fig. 4C,D). Due to the similarity of results in two independent KD cell lines of CtIP-CtBP1/2-HDAC1-AP1 components, we only used the KD1 cell lines for subsequent studies.

The CtIP-CtBP1/2-HDAC1-AP1 transcriptional complex specifically controlled the expression of four DNA damage and repair-related genes

The downstream targets of the CtBP1/2-HDAC1-AP1 transcriptional complex in osteosarcoma cells were identified by microarray analysis using RNA samples from Control-KD, CtIP-KD1, CtBP1-KD1 (all the KD cell lines were in the Saos2 background), Control-OE, CtIP-OE1, and CtBP1-OE1 (all the OE cell lines were in the hFOB1.19 background). Analysis of the differentially expressed genes in each cell line and comparison to control cells revealed 11 genes that were consistently overexpressed in both CtIP-KD1 and CtBP1-KD1 cells but were downregulated in both CtIP-OE1 and CtBP1-OE1 cells (Fig. 5A and Table S6). These 11 genes were *MLH1, MSH3, BRCA1*, growth factor receptor bound protein 2 (*GRB2*), chromodomain helicase DNA binding protein 4 (*CHD4*), *BAX*, metastasis associated 1 family member 2 (*MTA2*), deadbox helicase 5 (*DDX5*), DNA damage binding protein 2 (*DDB2*), ubiquitin like modifier activating enzyme 2 (*UBA2*), and *CDKN1A*. We found another 6 genes that were consistently downregulated in both CtIP-KD1 and CtBP1-KD1 cells but overexpressed in both CtIP-OE1 and CtBP1-OE1 cells (Fig. 5A and Table S6). These 6 genes were mouse double minute 4 (*MDM4*), cyclin E1 (*CCNE1*), nucleotide binding protein 2 (*NUBP2*), mitofusin 2 (*MFN2*), sorting nexin 9 (*SNX9*), and ribonucleic acid export 1 (*RAE1*).

We also determined whether these 17 genes were targets of the AP1 transcription factor by first analyzing the promoter sequences (2000 bp length) of all 17 genes using the AP1 consensus sequence TGAG/CTCA to

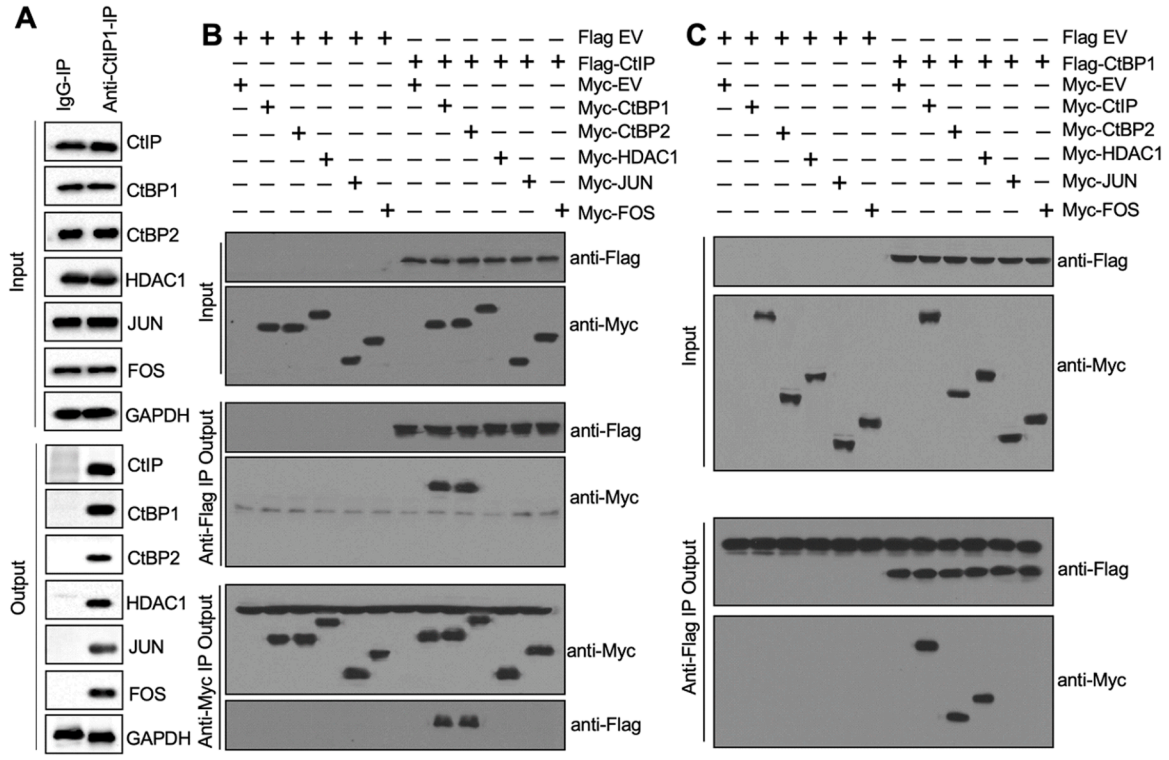

Fig. 3. *The formation of the CtIP-CtBP1/2-HDAC1-AP1 complex in vivo and in vitro* **(A)** CtIP immunoprecipitated CtBP1, CtBP2, HDAC1, JUN, and FOS. Three independent tumor tissues with equal weights (0.1 g) were mixed and then homogenized. The CtIP-purified complex in the homogenate was probed with antibodies indicated in the figure. **(B** and **C)** Co-IP results. Different combinations of vectors were co-transfected into Saos2 cells, and IP assays were performed using anti-Flag and anti-Myc agarose beads. The input and output proteins were probed with anti-Flag and anti-Myc, respectively. **(B)** CtIP directly interacted with CtBP1/2 *in vitro*. **(C)** CtBP1 directly interacted with CtIP, CtBP2, and HDAC1 *in vitro*. All data in this figure were independently repeated in triplicates and one representative blot is shown.

identify the AP1 binding sites. Only four gene promoters, *MLH1, MSH3, BRCA1*, and *CDKN1A*, contained an AP1 binding site (Fig. 5B). This result implied that the other 13 genes might not be direct targets of AP1. We confirmed this by determining the mRNA levels of all 17 genes in Control-KD, CtIP1-KD, CtBP1-KD, CtBP2-KD, HDAC1-KD, JUN-KD, and FOS-KD cells (Saos2 background). The qRT-PCR results indicated that the depletion of CtIP and CtBP1/2 affected the expression of all 17 genes (Figs. S5 and S6), in agreement with the microarray results. HDAC1 deficiency induced *MLH1, MSH3, BRCA1, GRB2, CHD4, BAX, DDX5, DDB2*, and *CDKN1A* expression, but suppressed *MFN2* expression (Figs. S5 and S6). HDAC1 deficiency did not affect the expression of *MTA2, UBA2, MDM4, CCNE1, NUBP2, SNX9*, or *RAE1* (Figs. S5 and S6). Knockdown of the AP1 subunits only affected the expression of *MLH1, MSH3, BRCA1*, and *CDKN1A*, but not the other genes (Figs. S5 and S6). Comparison of the expression patterns of these four genes in CtIP-KD, CtBP-KD, and HDAC1-KD cells versus AP1-KD cells revealed that knockdown of CtIP, CtBP1/2, or HDAC1 increased *MLH1, MSH3, BRCA1*, and *CDKN1A* expression, whereas AP1 subunit depletion decreased the expression of these genes (Figs. S5 and S6). These results indicated that CtIP, CtBP1/2, and HDAC1 served as negative transcription regulators that mediated the expression of *MLH1, MSH3, BRCA1*, and *CDKN1A*.

We also examined the transcriptional regulation of the CtIP-CtBP1/2-HDAC1-AP1 complex in *MLH1, MSH3, BRCA1*, and *CDKN1A* by performing ChIP assays in the KD cells of CtIP-CtBP1/2-HDAC1-AP1 members using anti-CtIP, anti-CtBP1, anti-JUN, anti-FOS, and IgG (negative control). We selected 8 genes (*MLH1, MSH3, BRCA1, CDKN1A, GRB2, CHD4, BAX*, and *MAT2*) as representatives to determine the occupancies of CtIP-CtBP1/2-HDAC1-AP1 members on their promoters. The CtIP-CtBP1/2-HDAC1-AP1 complex specifically bound to the promoters of *MLH1, MSH3, BRCA1*, and *CDKN1A* but not to the promoters of *GRB2, CHD4, BAX*, or *MAT2* (Figs. S7–S10). Knockdown of any of the CtIP, CtBP1/2, HDAC1, or AP1 subunits decreased the occupancy of the complex on the promoters of *MLH1, MSH3, BRCA1*, and *CDKN1A* (Figs. S7 and S8). CtIP, CtBP1/2, and HDAC1 could bind to the promoters of *GRB2, CHD4*, and *BAX*, whereas AP1 could not (Figs. S9 and S10). Both CtIP and CtBP1/2 could bind to the promoter of *MAT2*, whereas HDAC1 and AP1 could not (Figs. S9 and S10).

Overexpression of MLH1/MSH3/BRCA1/CDKN1A in CtlP-KD, CtBP1/2-KD, and HDAC1-KD cells could be inhibited by double knockdown of JUN and FOS

The opposite regulation of *MLH1/MSH3/BRCA1/CDKN1A* by AP1 and the other four negative regulators **(**CtIP, CtBP1/2, and HDAC1) prompted us to investigate the effects of AP1 depletion in CtIP-KD1, CtBP1-KD1, CtBP2-KD1, and HDAC1-KD1 cells. We transfected JUN and FOS siRNAs into CtIP-KD1, CtBP1-KD1, CtBP2-KD1, and HDAC1-KD1 cells to generate triple-KD cells (Fig. S11A). We then measured the mRNA levels of *MLH1, MSH3, BRCA1*, and *CDKN1A* in those cells. The qRT-PCR results showed that double knockdown of JUN and FOS in CtIP-KD1, CtBP1-KD1, CtBP2-KD1, and HDAC1-KD1 cells significantly decreased the expression of *MLH1, MSH3, BRCA1*, and *CDKN1A* (Fig. S11B).

Four DNA damage repair genes were downregulated in both osteosarcoma biopsies and cells

We measured the expression levels of all four CtIP-CtBP1/2-HDAC1-AP1 targets involved in DNA damage repair in osteosarcoma biopsies and cells using the same RNA samples from 20 pairs of cancerous biopsies and their adjacent noncancerous tissues used in Fig. 1A. The qRT-

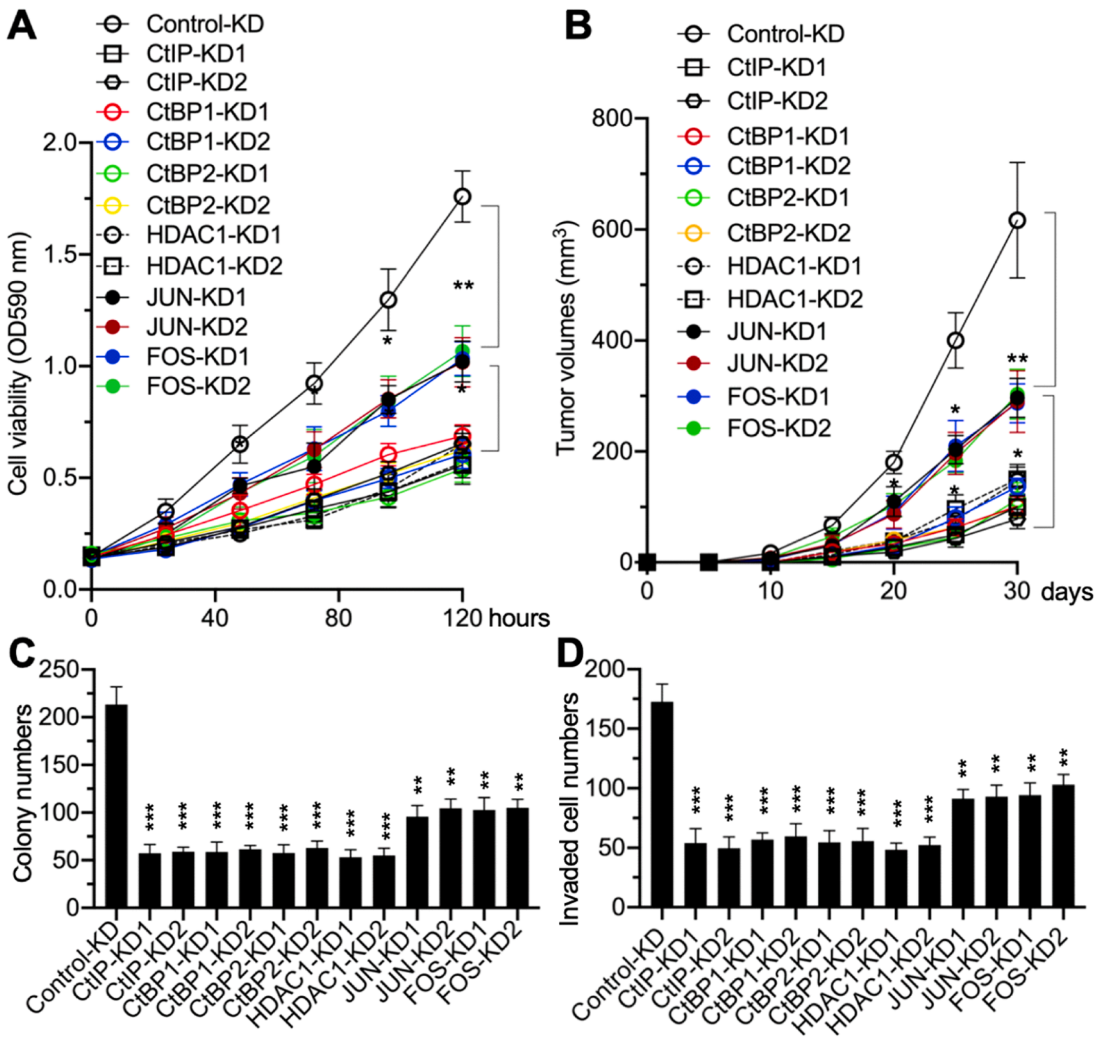

Fig. 4. *Depletion of CtIP and CtBPs decreased cell viability, colony formation, cell invasion, and tumor growth* **(A)** MTT assay results for CtIP-CtBP1/2-HDAC1-AP1 components in the knockdown cells. $^{*}P < 0.01$ and $^{**}P < 0.01$. **(B)** Tumor xenograft results for CtIP-CtBP1/2-HDAC1-AP1 components in the knockdown cells (for each cell line, 10 mice were injected). $^{*}P < 0.01$ and $^{**}P < 0.01$. Tumor volumes were measured at 5-day intervals. $^{***}P < 0.001$. **(C)** Colony numbers after cell culture (knockdown cells of individual CtIP-CtBP1/2-HDAC1-AP1 components) for 14 days. ns: no significance. $^{**}P < 0.01$ and $^{***}P < 0.001$. **(D)** Invaded cell numbers in Boyden chamber assays. ns: no significance. $^{**}P < 0.01$ and $^{***}P < 0.001$. All data in this figure are presented as the mean ± SD of three independent experiments.

PCR analyses showed that *MLH1, MSH3, BRCA1*, and *CDKN1A* were all downregulated *in vivo* (Fig. 6A–D). In contrast to CtIP, we found that the expression levels of *MLH1, MSH3, BRCA1*, and *CDKN1A* in MG63, KHOS, 143B, HOS, Saos2, and U2OS cells were decreased to varying degrees (Fig. 6E).

Overexpression of four DNA damage repair genes in osteosarcoma cells decreased cell viability, colony formation, cell invasion, and tumor volumes

We explored the contribution of individual DNA damage and repair genes in osteosarcoma cells by overexpressing pCDNA3-Flag empty vector, pCDNA3-Flag-MLH1, pCDNA3-Flag-MSH3, pCDNA3-Flag-BRCA1, and pCDNA3-Flag-CDKN1A in Saos2 cells to generate Control-OE, MLH1-OE, MSH3-OE, BRCA1-OE, and CDKN1A-OE cells, respectively (Fig. S12). Cell viability assays showed that overexpression of *MLH1, MSH3, BRCA1*, or *CDKN1A* slightly decreased cell viability, but the viability was higher than in the CtIP-KD1 cells (Fig. 7A).

Injection of these cells into C57BL/6 mice ($n = 10$ for each cell line) to generate tumors revealed that the tumors in mice harboring MLH1-OE, MSH3-OE, BRCA1-OE, or CDKN1A-OE cells did not differ significantly in size, but they were smaller than the tumors in mice harboring Control-OE cells and were larger than in mice injected with CtIP-KD1 cells (Fig. 7B). We determined the colony formation and cell invasion using the same cells and again found that overexpression of *MLH1, MSH3, BRCA1*, or *CDKN1A* decreased the numbers of colonies formed, as well as the extent of cell invasion (Fig. 7C,D).

Discussion

The uncontrolled DNA damage and repair process is an important cause that leads to tumorigenesis [23]. Disruption of DNA repair related genes, such as *MLH1, MSH3, BRCA1*, and *CDKN1A*, has been identified to contribute to tumorigenesis through different DNA repair mechanisms [24,25]. However, the underlying mechanisms of these gene dysregulations are still obscure. In the current study, we confirmed a requirement for the CtIP-CtBP1/2-HDAC1-AP1 complex for the transcriptional suppression of *MLH1, MSH3, BRCA1*, and *CDKN1A* in the process of osteosarcoma tumorigenesis (Fig. 8).

DNA can be damaged by irradiation, reactive oxygen species (ROS), and chemical reagents [26]. Once DNA damage occurs, eukaryotic organisms initiate the DNA repair system to remove the damaged DNA

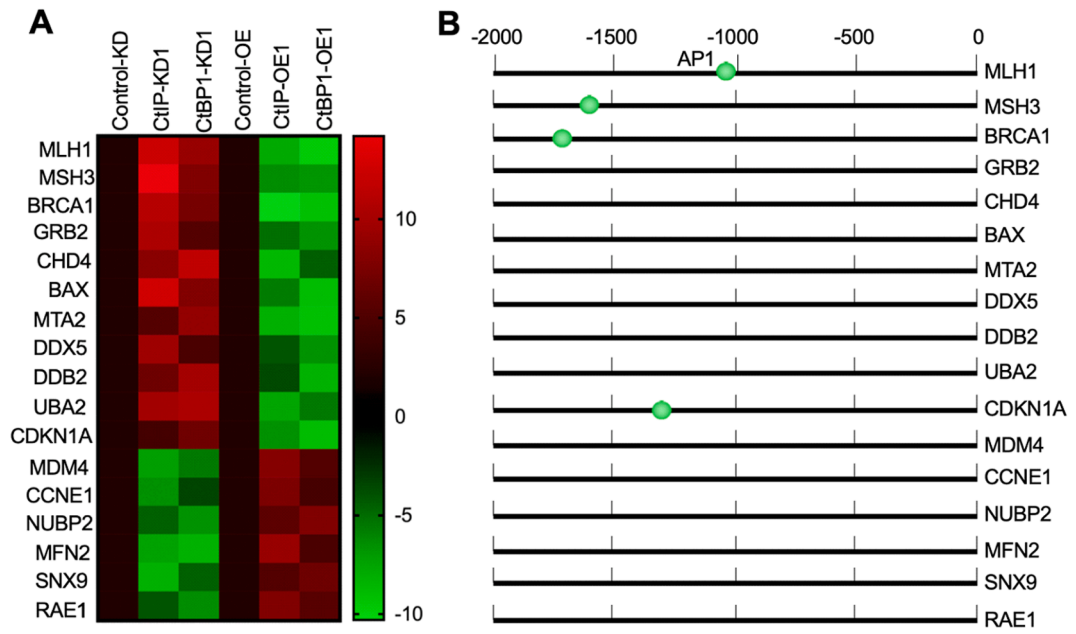

Fig. 5. *Identification of CtIP-CtBP1/2-HDAC1-AP1 downstream targets by microarray analysis and conserved AP1 consensus sequence* **(A)** Microarray results. RNA samples from Control-KD, CtIP-KD1, and CtBP1-KD1 cells (in Saos2 background), as well as Control-OE, CtIP-OE, and CtBP1-OE cells (in hFOB1.19 background) were subjected to microarray analysis. Genes that were consistently dysregulated in CtIP-KD1 and CtBP1-KD1 but conversely expressed in CtIP-OE and CtBP1-OE cells are presented. Data are presented as the mean ± SD of three independent experiments. **(B)** Prediction of AP1 binding sites on the promoters of potential target genes of CtIP-CtBP1/2-HDAC1-AP1. The promoters (2000 bp length in the upstream of ATG) of the genes shown in the figure were used to identify the AP1 binding sites (TGAG/CTCA).

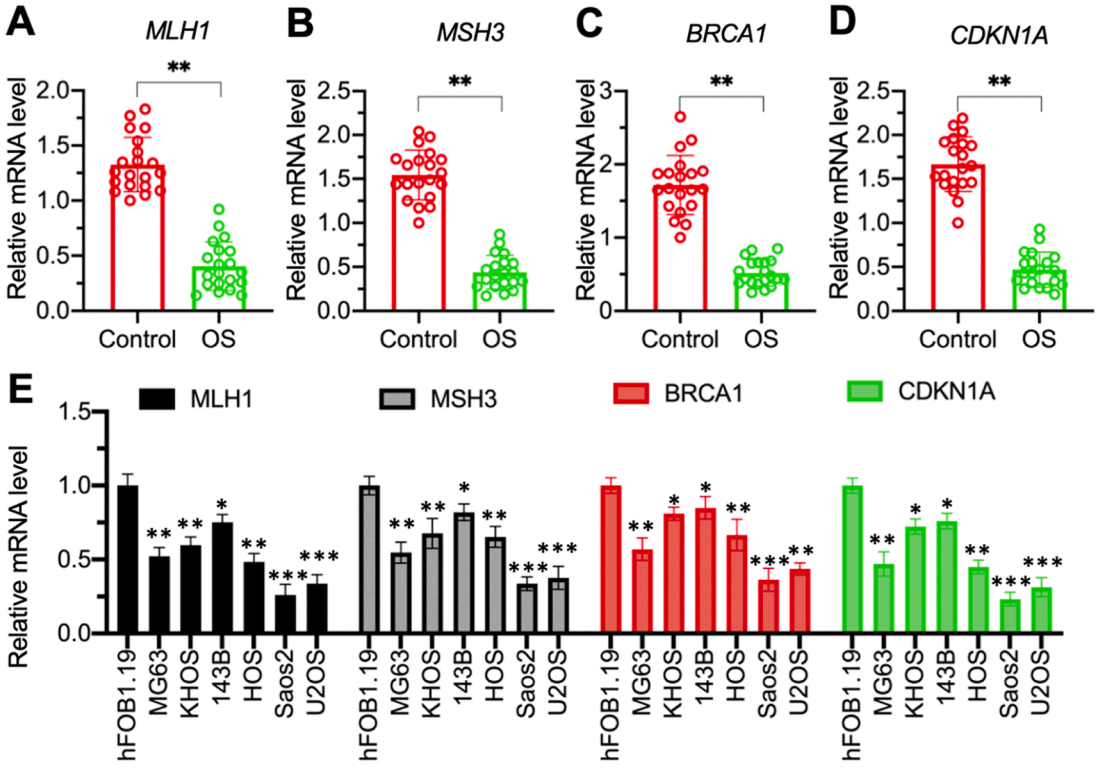

Fig. 6. *The mRNA levels of MLH1, MSH3, BRCA1, and CDKN1A in osteosarcoma tumor tissues and cell lines* **(A–D)** The mRNA levels of *MLH1, MSH3, BRCA1*, and *CDKN1A* in osteosarcoma tumor tissues ($n = 20$). The same RNA samples as shown in Fig. 1A were used for qRT-PCR analysis to measure the mRNA levels of *MLH1* **(A)**, *MSH3* **(B)**, *BRCA1* **(C)**, and *CDKN1A* **(D)**. $^{**}P < 0.01$. **(E)** The mRNA levels of *MLH1, MSH3, BRCA1*, and *CDKN1A* in 6 osteosarcoma cell lines (MG63, KHOS, 143B, HOS, Saos2, and U2OS). $^{*}P < 0.05$, $^{**}P < 0.01$, and $^{***}P < 0.001$. All data in this figure are presented as the mean ± SD of three independent experiments.

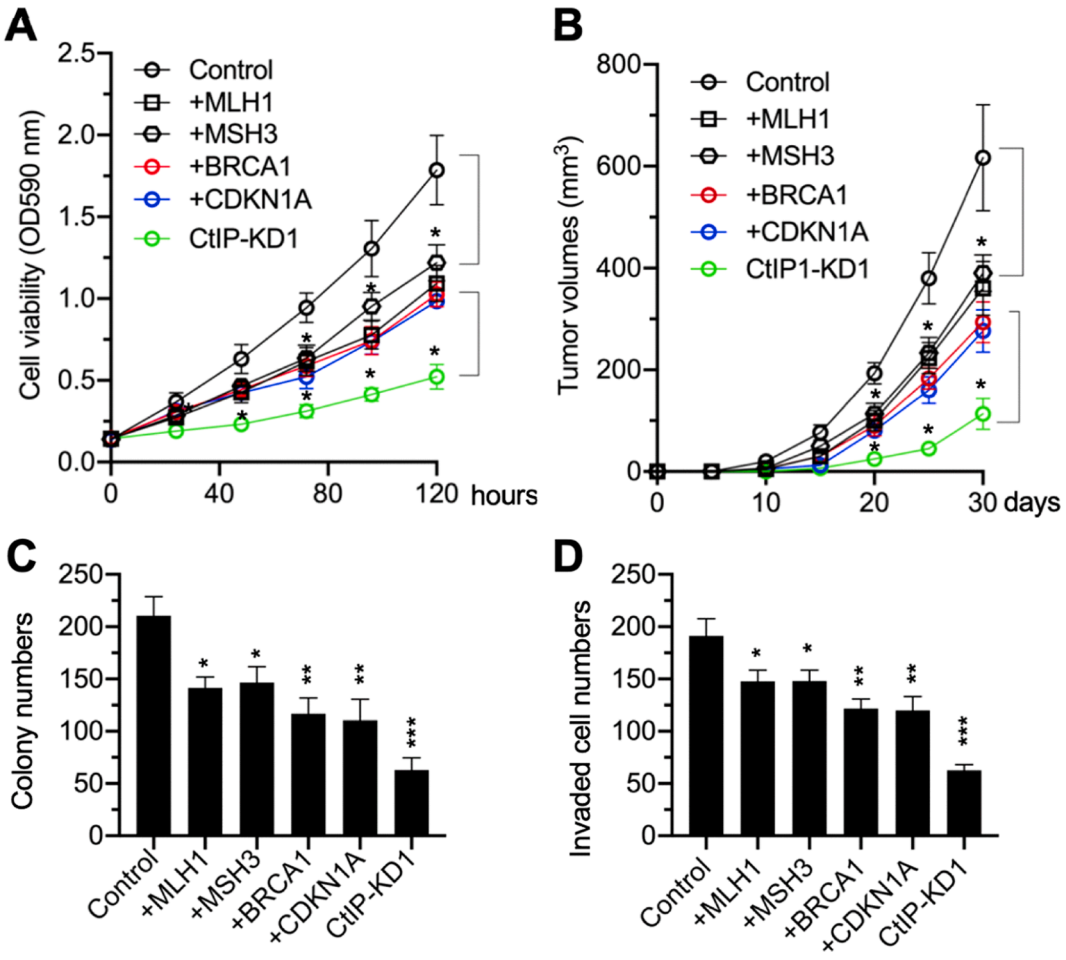

Fig. 7. *Overexpression of MLH1/MSH3/BRCA1/CDKN1A decreased osteosarcoma cell viability, colony formation, cell invasion, and tumor growth* **(A)** MTT assay results in cells overexpressing *MLH1/MSH3/BRCA1/CDKN1A*. Saos2 cells expressing pCDNA3-Flag (Control), pCDNA3-Flag-MLH1, pCDNA3-Flag-MSH3, pCDNA3-Flag-BRCA1 or pCDNA3-Flag-CDKN1A were subjected to MTT assays to determine cell viability. $^{*}P < 0.05$. **(B)** Tumor xenograft results using cells overexpressing *MLH1/MSH3/BRCA1/CDKN1A* (for each cell line, 10 mice were injected). Tumor volumes were measured at 5-day intervals. $^{*}P < 0.05$. **(C)** Colony numbers after culture of cells overexpressing *MLH1/MSH3/BRCA1/CDKN1A* for 14 days. ns: no significance. $^{*}P < 0.05$ and $^{**}P < 0.01$. **(D)** Invaded cell numbers in the Boyden chamber assay. ns: no significance. $^{*}P < 0.05$, $^{**}P < 0.01$, and $^{***}P < 0.001$. All data in this figure are presented as the mean ± SD of three independent experiments.

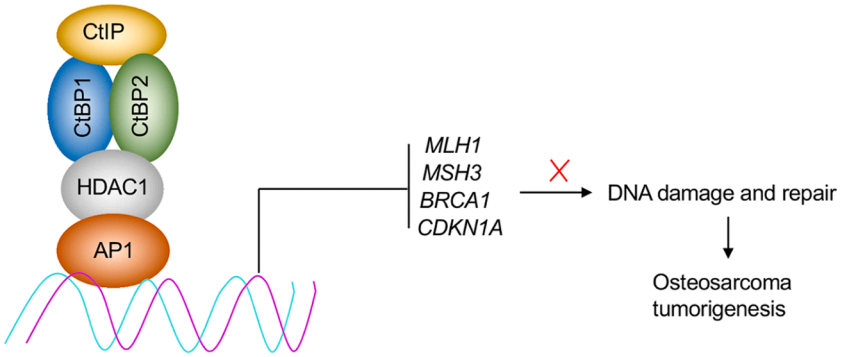

Fig. 8. *A schematic diagram of the assembly of the CtIP-CtBP1/2-HDAC1-AP1 complex and its role in osteosarcoma tumorigenesis* Overexpressed CtIP couples with CtBP1/2 heterodimer, HDAC1, and AP1 subunits to assemble a transcriptional complex. This complex binds to the promoters of *MLH1, MSH3, BRCA1*, and *CDKN1A* to repress their expression. The downregulation of these genes impairs the DNA repair process and increases genome stability, causing tumorigenesis.

[27]. This removal involves several different kinds of DNA repair pathways, such as base excision repair (BER), nucleotide excision repair (NER), mismatch repair (MMR), homologous recombination (HR), non-homologous end joining (NHEJ), and direct repair [27]. MLH1 is a tumor suppressor gene in multiple cancers, including colorectal cancer and prostate cancer [28,29], and mutation of MLH1 is also associated with osteosarcoma [30], but the molecular mechanism is not known.

MLH1 participates in MMR by assembly of a complex with Post-meiotic Segregation Increased 2 (PMS2) [31]. In addition to *MLH1* and *PMS2*, the human genome encodes 5 other MMR genes: *MLH3, MSH2, MSH3, MSH6*, and *PMS1* [24]. DNA repair is initiated after sensing the assembly of MSH2-MSH6 or MSH2-MSH3 heterodimer [24]. These two

heterodimers then recruit the MLH1-PMS2 complex to repair the mismatched DNA [24].

BRCA1 is a well-known tumor suppressor protein in cancers, and especially in breast and ovarian cancers [32]. Exosome sequencing reveals that BRCA1 and BRCA2 are deficient in over 80% of osteosarcomas [32]. BRCA1 promotes the repair of damaged DNA to maintain genome stability and suppress tumorigenesis by both the NHEJ and HR pathways [32]. When DNA damage occurs, BRCA1 interacts with PALB2 (partner and localizer of BRCA2) and recruits the RAD51/BRCA2 complex to the DSB sites to initiate DNA repair [33].

CDKN1A is also a well-characterized tumor suppressor, and its deficiency can cause cell cycle arrest and impair the DNA repair process [34]. Experimental evidence has confirmed that CDKN1A interacts with PCNA (proliferating cell nuclear antigen) and is directly involved in DNA repair by mediating NER and BER [34]. In the present study, *MLH1, MSH3, BRCA1*, and *CDKN1A* were downregulated in osteosarcoma cells and suppressed by the CtIP-CtBP1/2-HDAC1-AP1 complex. However, the focus of this study was not on the downstream signaling pathways of *MLH1, MSH3, BRCA1*, and *CDKN1A*. The impairment of these four genes implies that multiple DNA repair pathways drive chromosomal instability during osteosarcoma tumorigenesis and that the CtIP-CtBP1/2-HDAC1-AP1 complex could be therapeutically exploited. Intriguingly, we found that the depletion of CtIP, CtBP1/2, and HDAC1 may cause DNA double-strand break (DSB) in CtIP-KD1, CtBP1-KD1, CtBP2-KD1, and HDAC1-KD1 cells because we observed the induction of the phosphorylated H2A histone family member X (γH2AX) (Fig. S13), a sensitive molecular marker of DNA damage and repair [35]. Although we still do not know the underlying mechanisms regarding this phenomenon, we assume that one possibility is that the depletion of CtIP, CtBP1/2, and HDAC1 instead of AP1 leads to the accumulation of ROS, resulting in the generation of DSB. ROS is an important trigger that leads to DSB [36]. Among *MLH1, MSH3, BRCA1*, and *CDKN1A* genes, overexpression of *CDKN1A* can increase intracellular ROS level [37]. In addition, *DDB2*, an upregulated gene in CtIP-KD1, CtBP1-KD1, CtBP2-KD1, and HDAC1-KD1 cells instead of AP1-KD cells (Fig. S6), can also positively regulate ROS level [38]. Therefore, the growth inhibition in CtIP-KD1, CtBP1-KD1, CtBP2-KD1, and HDAC1-KD1 cells is probably the counteracting effects of overexpression of DNA repair genes and DSB. More data are required to demonstrate the mechanism of DSB occurrence and the coeffects of DSB and upregulation of DNA repair genes in the future.

One interesting finding in this study is the transrepression of *BRCA1* by CtIP. Previous studies have shown that BRCA1 is a downstream target of CtBP1 and that it can directly interact with CtIP in the G2 phase of the cell cycle [39]. We found that CtIP couples with the CtBP1/2 heterodimer to suppress the expression of *BRCA1* by binding to its promoter. Although we did not examine the direct interaction between BRCA1 and CtIP in osteosarcoma cells, BRCA1 was not observed in the candidates of CtIP-associated proteins identified by mass spectrometry analysis. This result suggests that CtIP may not broadly interact with BRCA1 in the tumorigenesis of osteosarcoma.

AP1 subunits, especially FOS, are widely involved in bone formation, resorption, and osteoclast differentiation [40]. Moreover, FOS has been reported to function as an oncogene and it is overexpressed in the majority of human osteosarcoma [41]. FOS cooperates with JUN to induce osteosarcoma formation in mice [42]. Although AP1 and the other four regulators (CtIP, CtBP1, CtBP2, and HDAC1) had opposite effects on the regulation of *MLH1, MSH3, BRCA1*, and *CDKN1A*, we observed that depletion of AP1 subunits also decreased cell viability, colony numbers, cell invasion, and tumor volumes in mice (Fig. 4). One reasonable explanation for this phenomenon is that AP1 can mediate the expression of numerous genes involved in tumorigenesis, metastasis, and angiogenesis. For instance, AP1 can activate the expression of fibroblast growth factor receptor 1 (*FGFR1*) and promote metastasis in osteosarcoma [43]. Overexpression of FOS in osteoblasts induces the expression of cyclin A (*CCNA1*) to accelerate cell cycle progression [44]. In osteosarcoma cells, phosphorylated FOS and FOS-related antigen 1 (Fra1) can induce the expression of *MMP1* [45], which is required for cell invasion and epithelial-mesenchymal transition (EMT). Thus, depletion of AP1 in human osteosarcoma cells may cause diverse effects beyond just affecting the expression of *MLH1, MSH3, BRCA1*, and *CDKN1A*.

In addition to these DNA repair related genes, we found another 13 genes that were controlled by CtIP and CtBP1/2 but not by AP1. Among these 13 genes, some also contribute to tumorigenesis. For instance, GRB2 is overexpressed in breast cancer cells, and it functions as a mediator of ErbB2 (epidermal growth factor receptor 2) signaling to affect oncogenesis [46]. CHD4 is overexpressed in multiple tumors, and it can affect tumor cell migration and invasion [47]. BAX is a critical cell death regulator, and it functions as a tumor suppressor in osteosarcoma by inhibiting apoptosis signaling [8]. Although these genes were not regulated by AP1, they are all the targets of CtIP-CtBP1/2 and they may be controlled by other transcriptional complexes assembled by different transcription factors with CtIP-CtBP1/2.

In summary, we verified that CtIP couples with CtBP1/2 heterodimer, HDAC1, and two subunits of AP1 transcription factor to form a transcriptional complex that is required for the transrepression of four DNA damage and repair-related genes, namely *MLH1, MSH3, BRCA1*, and *CDKN1A*. We also found that a deficiency of the CtIP-CtBP1/2-HDAC1-AP1 complex in osteosarcoma cells increased the expression of *MLH1, MSH3, BRCA1*, and *CDKN1A*, thereby activating the DNA damage and repair process and inhibiting osteosarcoma cell growth.

Ethical approval statement

All experimental procedures used in this study were performed in accordance with the approved guidelines of the ethical board of Xi'an Jiaotong University College of Medicine.

CRediT authorship contribution statement

Xun Chen: Methodology, Resources. **Qian Zhang:** Methodology, Investigation. **Xiaoqian Dang:** Methodology, Investigation. **Jinzhu Fan:** Methodology, Investigation. **Tao Song:** Methodology, Investigation. **Zhong Li:** Methodology, Investigation. **Ning Duan:** Visualization, Formal analysis, Writing – original draft. **Wentao Zhang:** Visualization, Formal analysis, Writing – original draft.

Declaration of Competing Interest

The authors declare that they have no competing financial or nonfinancial interests that might have influenced the performance or presentation of the work described in this manuscript.

Acknowledgment

This work was supported by a grant from Natural Science Foundation of Shaanxi Province, China (Grant No. 2020JM-688).

Supplementary materials

Supplementary material associated with this article can be found, in the online version, at doi:10.1016/j.tranon.2022.101429.

References

[1] S.J. Taran, R. Taran, N.B. Malipatil, Pediatric osteosarcoma: an updated review, Indian J. Med. Paediatr. Oncol. 38 (2017) 33–43.
[2] D.R. Reed, M. Hayashi, L. Wagner, O. Binitie, D.A. Steppan, A.S. Brohl, et al., Treatment pathway of bone sarcoma in children, adolescents, and young adults, Cancer 123 (2017) 2206–2218.
[3] M.L. Broadhead, J.C. Clark, D.E. Myers, C.R. Dass, PF. Choong, The molecular pathogenesis of osteosarcoma: a review, Sarcoma 2011 (2011), 959248.

[4] A.M. Czarnecka, K. Synoradzki, W. Firlej, E. Bartnik, P. Sobczuk, M. Fiedorowicz, et al., Molecular biology of osteosarcoma, Cancers 12 (2020) 2130 (Basel).
[5] Z. Chen, The transrepression and transactivation roles of CtBPs in the pathogenesis of different diseases, J. Mol. Med. 99 (2021) 1335–1347 (Berl).
[6] G. Chinnadurai, CtBP, an unconventional transcriptional corepressor in development and oncogenesis, Mol. Cell 9 (2002) 213–224.
[7] M.A. Blevins, M. Huang, R. Zhao, The role of CtBP1 in oncogenic processes and its potential as a therapeutic target, Mol. Cancer Ther. 16 (2017) 981–990.
[8] C. Li, X.Q. Xiao, Y.H. Qian, Z.Y. Zhou, The CtBP1-p300-FOXO3a transcriptional complex represses the expression of the apoptotic regulators Bax and Bim in human osteosarcoma cells, J. Cell. Physiol. 234 (2019) 22365–22377.
[9] S.K. Ray, H.J. Li, E. Metzger, R. Schule, A.B. Leiter, CtBP and associated LSD1 are required for transcriptional activation by *NEUROD1* in gastrointestinal endocrine cells, Mol. Cell. Biol. 34 (2014) 2308–2317.
[10] L.D. Boxer, B. Barajas, S. Tao, J. Zhang, PA. Khavari, ZNF750 interacts with KLF4 and RCOR1, KDM1A, and CTBP1/2 chromatin regulators to repress epidermal progenitor genes and induce differentiation genes, Genes Dev. 28 (2014) 2013–2026.
[11] X. Chen, Q. Zhang, X. Dang, T. Song, Y. Wang, Z. Yu, et al., Targeting the CtBP1-FOXM1 transcriptional complex with small molecules to overcome *MDR1*-mediated chemoresistance in osteosarcoma cancer stem cells, J. Cancer 12 (2021) 482–497.
[12] N.L. Mozaffari, F. Pagliarulo, A.A. Sartori, Human CtIP: a 'double agent' in DNA repair and tumorigenesis, Semin. Cell Dev. Biol. 113 (2021) 47–56.
[13] A. Syed, J.A. Tainer, The MRE11-RAD50-NBS1 complex conducts the orchestration of damage signaling and outcomes to stress in DNA replication and repair, Annu. Rev. Biochem. 87 (2018) 263–294.
[14] R. Anand, L. Ranjha, E. Cannavo, P. Cejka, Phosphorylated CtIP functions as a co-factor of the MRE11-RAD50-NBS1 endonuclease in DNA end resection, Mol. Cell 64 (2016) 940–950.
[15] Y. Yu, L. Chen, G. Zhao, H. Li, Q. Guo, S. Zhu, et al., RBBP8/CtIP suppresses P21 expression by interacting with CtBP and BRCA1 in gastric cancer, Oncogene 39 (2020) 1273–1289.
[16] F. Oswald, M. Winkler, Y. Cao, K. Astrahantseff, S. Bourteele, W. Knochel, et al., RBP-Jkappa/SHARP recruits CtIP/CtBP corepressors to silence Notch target genes, Mol. Cell. Biol. 25 (2005) 10379–10390.
[17] N. Duan, W. Zhang, T. Song, Z. Li, X. Chen, W. Ma, A naturally derived small molecule PSM0537 targets the AF1Q-TCF4 interaction to suppress COX2 expression and inhibit cell proliferation and metastasis in osteosarcoma, Am. J. Cancer Res. 11 (2021) 2637–2653.
[18] J. Ren, Y. Wu, Y. Wang, Y. Zhao, Y. Li, S. Hao, et al., CtIP suppresses primary microRNA maturation and promotes metastasis of colon cancer cells in a xenograft mouse model, J. Biol. Chem. 296 (2021), 100707.
[19] Y. Shi, J. Sawada, G. Sui, B. Affarel, J.R. Whetstine, F. Lan, et al., Coordinated histone modifications mediated by a CtBP co-repressor complex, Nature 422 (2003) 735–738.
[20] X. Zhang, K. Du, Z. Lou, K. Ding, F. Zhang, J. Zhu, et al., The CtBP1-HDAC1/2-IRF1 transcriptional complex represses the expression of the long noncoding RNA GAS5 in human osteosarcoma cells, Int. J. Biol. Sci. 15 (2019) 1460–1471.
[21] L.J. Zhao, M. Kuppuswamy, S. Vijayalingam, G. Chinnadurai, Interaction of ZEB and histone deacetylase with the PLDLS-binding cleft region of monomeric C-terminal binding protein 2, BMC Mol. Biol. 10 (2009) 89.
[22] M.L. Mittelstadt, R.C. Patel, AP-1 mediated transcriptional repression of matrix metalloproteinase-9 by recruitment of histone deacetylase 1 in response to interferon beta, PLoS One 7 (2012) e42152.
[23] P.A. Jeggo, L.H. Pearl, A.M. Carr, DNA repair, genome stability and cancer: a historical perspective, Nat. Rev. Cancer 16 (2016) 35–42.
[24] GM. Li, Mechanisms and functions of DNA mismatch repair, Cell Res. 18 (2008) 85–98.
[25] M. Tarsounas, P. Sung, The antitumorigenic roles of BRCA1-BARD1 in DNA repair and replication, Nat. Rev. Mol. Cell Biol. 21 (2020) 284–299.
[26] J. Cadet, J.R. Wagner, DNA base damage by reactive oxygen species, oxidizing agents, and UV radiation, Cold Spring Harb. Perspect. Biol. 5 (2013) a012559.
[27] N. Chatterjee, G.C. Walker, Mechanisms of DNA damage, repair, and mutagenesis, Environ. Mol. Mutagen. 58 (2017) 235–263.
[28] M. Sharma, Z. Yang, H. Miyamoto, Loss of DNA mismatch repair proteins in prostate cancer, Medicine 99 (2020) e20124 (Baltimore).
[29] S.A. Martin, C.J. Lord, A. Ashworth, Therapeutic targeting of the DNA mismatch repair pathway, Clin. Cancer Res. 16 (2010) 5107–5113.
[30] X. Chen, A. Bahrami, A. Pappo, J. Easton, J. Dalton, E. Hedlund, et al., Recurrent somatic structural variations contribute to tumorigenesis in pediatric osteosarcoma, Cell Rep. 7 (2014) 104–112.
[31] S. Richman, Deficient mismatch repair: read all about it (review), Int. J. Oncol. 47 (2015) 1189–1202.
[32] M. Kovac, C. Blattmann, S. Ribi, J. Smida, N.S. Mueller, F. Engert, et al., Exome sequencing of osteosarcoma reveals mutation signatures reminiscent of BRCA deficiency, Nat. Commun. 6 (2015) 8940.
[33] S.M. Sy, M.S. Huen, J. Chen, PALB2 is an integral component of the BRCA complex required for homologous recombination repair, Proc. Natl. Acad. Sci. U. S. A. 106 (2009) 7155–7160.
[34] O. Cazzalini, A.I. Scovassi, M. Savio, L.A. Stivala, E. Prosperi, Multiple roles of the cell cycle inhibitor p21(CDKN1A) in the DNA damage response, Mutat. Res. 704 (2010) 12–20.
[35] L.J. Mah, A. El-Osta, T.C. Karagiannis, gammaH2AX: a sensitive molecular marker of DNA damage and repair, Leukemia 24 (2010) 679–686.
[36] V. Sharma, L.B. Collins, T.H. Chen, N. Herr, S. Takeda, W. Sun, et al., Oxidative stress at low levels can induce clustered DNA lesions leading to NHEJ mediated mutations, Oncotarget 7 (2016) 25377–25390.
[37] S. Macip, M. Igarashi, L. Fang, A. Chen, Z.Q. Pan, S.W. Lee, et al., Inhibition of p21-mediated ROS accumulation can rescue p21-induced senescence, EMBO J. 21 (2002) 2180–2188.
[38] N. Roy, S. Bagchi, P. Raychaudhuri, Damaged DNA binding protein 2 in reactive oxygen species (ROS) regulation and premature senescence, Int. J. Mol. Sci. 13 (2012) 11012–11026.
[39] X. Yu, J. Chen, DNA damage-induced cell cycle checkpoint control requires CtIP, a phosphorylation-dependent binding partner of BRCA1 C-terminal domains, Mol. Cell. Biol. 24 (2004) 9478–9486.
[40] E.F. Wagner, R. Eferl, Fos/AP-1 proteins in bone and the immune system, Immunol. Rev. 208 (2005) 126–140.
[41] J.X. Wu, P.M. Carpenter, C. Gresens, R. Keh, H. Niman, J.W. Morris, et al., The proto-oncogene c-Fos is over-expressed in the majority of human osteosarcomas, Oncogene 5 (1990) 989–1000.
[42] Z.Q. Wang, J. Liang, K. Schellander, E.F. Wagner, A.E. Grigoriadis, c-Fos-induced osteosarcoma formation in transgenic mice: cooperativity with c-Jun and the role of endogenous c-Fos, Cancer Res. 55 (1995) 6244–6251.
[43] D. Weekes, T.G. Kashima, C. Zandueta, N. Perurena, D.P. Thomas, A. Sunters, et al., Regulation of osteosarcoma cell lung metastasis by the c-Fos/AP-1 target FGFR1, Oncogene 35 (2016) 2948.
[44] A. Sunters, D.P. Thomas, W.A. Yeudall, A.E. Grigoriadis, Accelerated cell cycle progression in osteoblasts overexpressing the c-Fos proto-oncogene: induction of cyclin A and enhanced CDK2 activity, J. Biol. Chem. 279 (2004) 9882–9891.
[45] R. Kimura, C. Ishikawa, T. Rokkaku, R. Janknecht, N. Mori, Phosphorylated c-Jun and Fra-1 induce matrix metalloproteinase-1 and thereby regulate invasion activity of 143B osteosarcoma cells, Biochim. Biophys. Acta 1813 (2011) 1543–1553.
[46] A. Giubellino, T.R. Burke, D.P. Bottaro, Grb2 signaling in cell motility and cancer, Expert Opin. Ther. Targets 12 (2008) 1021–1033.
[47] L. Xia, W. Huang, M. Bellani, M.M. Seidman, K. Wu, D. Fan, et al., CHD4 has oncogenic functions in initiating and maintaining epigenetic suppression of multiple tumor suppressor genes, Cancer Cell 31 (2017) 653–68e7.